Scanning Microscopy

Volume 1 | Number 3 Article 4

3-28-1987

Observation of Tungsten Field Emitter Tips with an Ultra-High Resolution Field Emission Scanning Electron Microscope

Katsuhiro Kuroda
Hitachi, Ltd.

Shigeyuki Hosoki
Hitachi, Ltd.

Tsutomu Komoda
Hitachi, Ltd.

Scanning Microscopy, Vol. 1, No. 3, 1987 (Pages 911-917)
Scanning Microscopy International, Chicago (AMF O'Hare), IL 60666 USA

0891-7035/87$3.00+.00

OBSERVATION OF TUNGSTEN FIELD EMITTER TIPS WITH AN ULTRA-HIGH RESOLUTION FIELD EMISSION SCANNING ELECTRON MICROSCOPE

Katsuhiro Kuroda*, Shigeyuki Hosoki, Tsutomu Komoda

Central Research Laboratory, Hitachi, Ltd.,
Kokubunji, Tokyo 185, Japan.

(Received for publication December 23, 1986, and in revised form March 28, 1987)

Abstract

Tungsten emitter tips are observed with a prototype scanning electron microscope with an approximate 5Å electron beam size at an accelerating voltage of 30kV. A field emission electron source and in-lens type objective lens are incorporated into the electron column. A special specimen stage was designed to clean the emitter tips using a flashing operation and to reduce contamination by heating them during the observation. The observed emitters were W<011>, W<001> and Ti/W<001>. The crystallographic planes were clearly visible in the W<011> and W<001> observation. It was also possible to observe atomic layer steps of 4.5Å during the recrystallization process by flashing operation of W<011>. In the observation of Ti/W, it was found that the aspect was quite different from that of the W<001> crystal surface. The observed field emission micrograph pattern was in good agreement with the tip shape.

Key Words: Ultra-high resolution, field emission electron source, in-lens type objective lens, tungsten field emitter tip, titaniated tungsten field emitter tip, crystallographic plane, atomic layer.

*Address For Correspondence:
Central Research Laboratory, Hitachi, Ltd., Kokubunji, Tokyo 185, Japan.
Phone No. 0423-23-1111(ext.3426)

Introduction

The resolution of scanning electron microscopes (SEM) has gradually become higher due to improvements in electron sources, electron optics, signal detectors and so on. Most notably, a field emission (FE) gun developed by Crewe et al. [2] has been used effectively for high resolution SEM because of its high brightness and low beam energy spread. Komoda et al. [4] developed the first FE-SEM with a resolution of 50Å at 20 kV in 1972, and Shimizu et al. [12] also developed another FE-SEM with almost the same resolution the following year. Since then, some improvements have been made to obtain even higher resolution. Nagatani et al.[11] improved the FE-SEM to reduce the working distance to zero and achieved a resolution of 15Å, and Tanaka [16] has taken many excellent images of a biological specimen using this SEM. Nagatani et al. [10] also tried to assemble the FE gun and an in-lens type objective lens [14] (specimens are positioned inside an objective lens) to obtain a resolution of about 10Å in 1983.

For a long time, the resolution limit in SEM was theoretically considered to be about 10 Å. This was based on the escape depth and a Monte Carlo calculation of the secondary electron distribution [5]. In references [16] and [17], it was indicated that this theoretical model was not perfectly applicable to low density biological materials covered with thin metal films. The model was made for a bulk specimen considered to be a semi-infinite solid of uniform density. Accordingly, if the SEM beam spot could be focused smaller, a higher resolution might be obtainable for low density material such as biological specimens.

To verify this hypothesis, the authors attempted to design an electron column of a prototype FE-SEM with an in-lens type objective lens to focus the electron beam as small as possible. The experimental results showed that the electron beam

could be focused as fine as 5Å from a scanning transmission electron image and an SEM resolution of approximately the same value was determined from the minimum separate distance between coated fine platinum particles [7]. Subsequently, Tanaka et al. [15] developed a UHS-T1 type SEM similar to the prototype SEM. Using this SEM at an accelerating voltage of 30 kV, they were able to confirm a resolution of 5Å. A recently available commercial version of the SEM Model S-900 guarantees a resolution of 8Å at 30 kV [9].

The authors [8] observed tungsten (W) FE tips as an application to show the high resolution capability of the prototype SEM, and showed the possibility of observing atomic layer steps of several angstroms. Subsequently, a titaniated W<001> (Ti/W) thermal FE tip was also observed, which was recently developed in our laboratory [3].

Column Construction

A schematic diagram of the electron column is shown in Fig. 1. A W<310> cold field emission electron gun is incorporated because of its high brightness and low beam energy spread. In the accelerating lens, a Butler-type anode system [1] is used in order to minimize aberration [6].

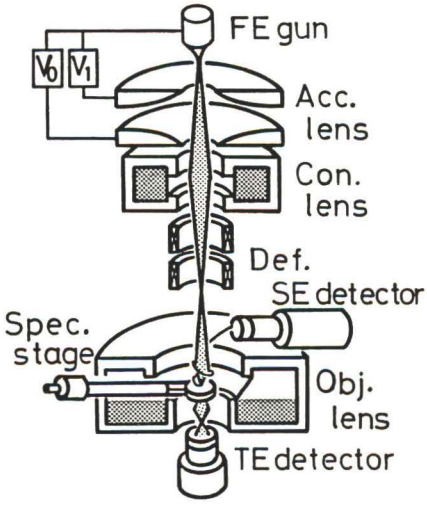

Fig. 1 Schematic diagram of electron column.

The gun and the anode system are followed by two magnetic lenses: a condenser and an objective lens. The condenser lens controls the demagnification and the beam current.

Specimens are positioned inside the objective lens to reduce aberration. The lens is the so-called in-lens type. The spherical and chromatic aberration coefficients of the lens are Cs=1.6mm and Cc=2.0mm, respectively. The beam spot size is mainly limited by spherical aberration and diffraction at accelerating voltages higher than 10 kV. Chromatic aberration and diffraction usually limit spot size reduction at voltages lower than 5 kV. The calculated characteristics of the beam spot size as a function of accelerating voltage are estimated as shown in Fig. 2. It is determined from this figure that a beam spot size of about 5Å can be obtained at 30 kV in this electron column.

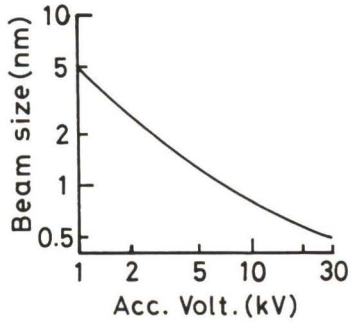

Fig. 2 Calculated electron optical characteristics: beam spot size varies according to accelerating voltages in the calculation.

Secondary electrons emitted from the specimen are picked up by an SE detector located between a pair of scanning deflectors and the objective lens, because the specimen is located inside the lens. Accordingly, a limiting aperture is used between the anode system and the condenser lens to avoid reducing the detectable efficiency of the secondary electrons. Moreover, a detector is placed below the objective lens so that electrons transmitted through the specimen can be used to form a scanning transmission electron (TE) image. The beam size is confirmed by analyzing this image.

The in-lens type objective lens restricts the capacity of the specimen chamber. The maximum specimen size is 20mmx6mmx2.4mm^t (X=±4mm, Y=±2mm). The tilt is 40°. The specimen stage is the side-entry type.

Specimen contamination is one of the most serious problems in high resolution SEM. Therefore, an oil-free evacuation system is used in the column. The column is evacuated with five ion-pumps. The pressure ultimately reaches 1×10^{-7} Pa in the gun chamber under normal operating conditions and is in the low 10^{-5} Pa range in the specimen chamber.

Observation for Tungsten FE-Tip

The SEM was used to observe W<011>, W<001> and Ti/W<001> field emitters. The Ti/W emitter was developed in our laboratory [3] and the monolayer of Ti is assumed to be adsorbed on the {100} plane. The authors tried to observe changes in the W<001> FE tip following thermal diffusion of Ti.

A special specimen stage was constructed in order to observe the emitters. The emitter tips were cleaned by flashing and contamination was reduced by heating the tips to several hundred degrees centigrade during the observations.

W<011> FE Tip

The W<011> emitter is made of a 0.1mm diameter polycrystalline wire. The wire is electrolytically etched and polished to form a needle-shaped <011> oriented tip as shown in Fig. 3. As the crystal planes cannot be observed in the tip immediately after etching, it is necessary to flash the tip at a high temperature in order to clean the crystal planes. The flashing also reforms the polycrystalline emitter tip into a single crystal through a recrystallization process.

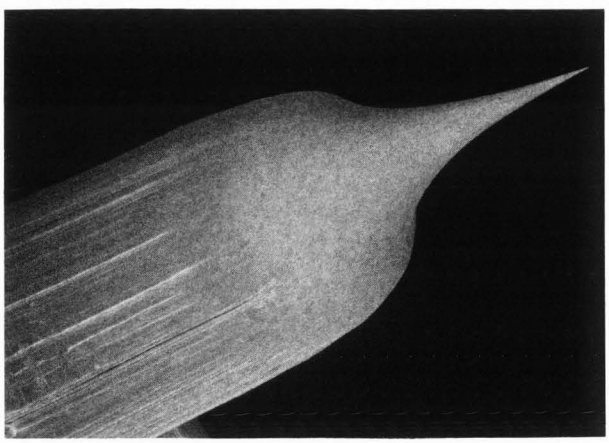

Fig. 3 Tungsten emitter image.

The tip image shown in Fig. 4 was taken after the tip had been flashed several times at 2000 ~ 2500 °C in 1 sec. bursts. Generally speaking, when an emitter is recrystallized, a clean pattern can be observed in a field emission micrograph (FEM). Since the observed emitter registered a clean FEM pattern, the tip was considered to be completely recrystallized.

A hemispherical model of a body centered cubic (bcc) structure is shown in Fig. 5, which has been made as spherical as possible. As each ball represents an atom, the scale of the model is about 1/20 of the observed tip size. The shape of each crystallographic plane in the actual emitter tip image is well defined when compared to the model. The [110], [211], [111] and [100] faces are hexagonal, striped, triangular and circular, respectively, in each micrograph. Thus, the sufficiently flashed and completely recrystallized tip is considered to be nearly hemispherical.

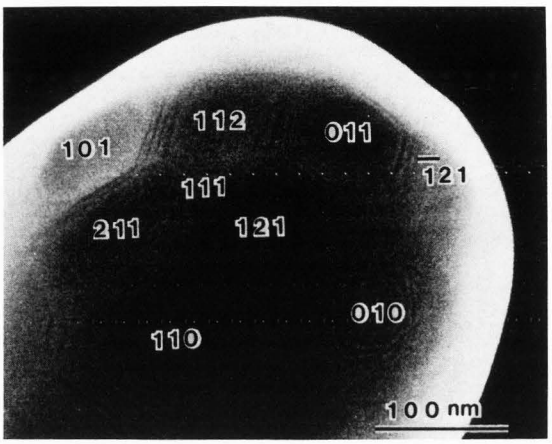

Fig. 4 Tungsten <110> emitter tip image. Each number shows Miller indices (hkl).

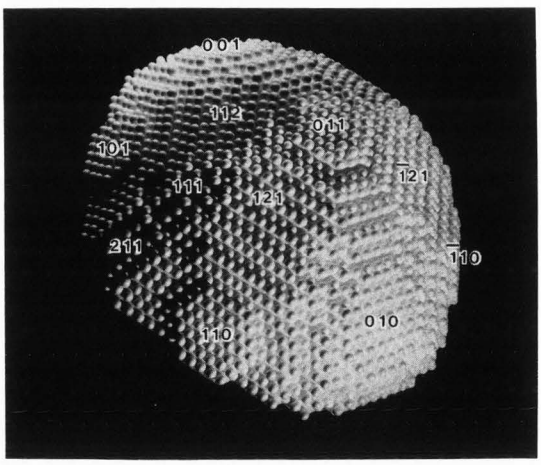

Fig. 5 Hemispherical model of bcc structure.

The atomic layer steps in Fig. 6-(b) are seen during the recrystallization process of a single crystal after weak flashing operations (1500 ~ 2000°C for 1sec. bursts). The image was taken with a direct magnification of 750,000. The reason for the incomplete recrystallization is thought to occur as follows. Crystallization usually begins from {110} which is the most stable lattice plane, and the steps of the {110} plane continuously build up to {210}, {111} and

so on. A {100} plane containing no step elements of the {110} plane is finally formed. As the emitter in Fig. 6 is not completely recrystallized, some crystallographic planes such as {110} and {211} are almost completely developed whereas the (010) plane is not formed.

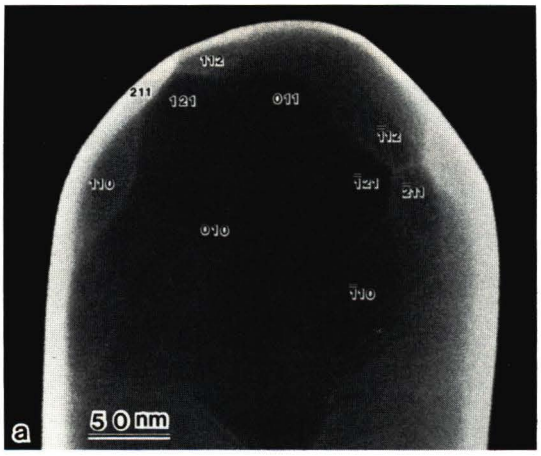

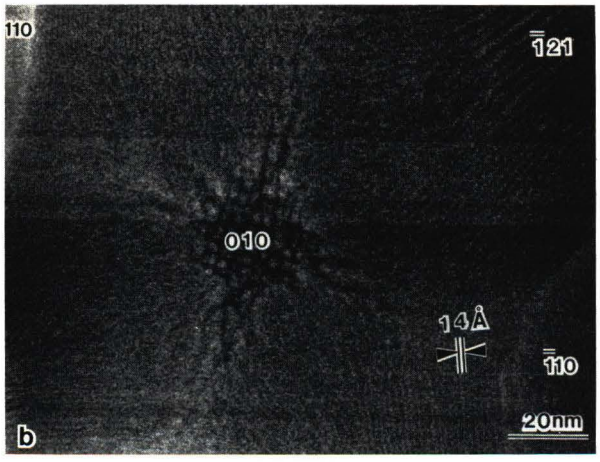

Fig. 6 Tungsten <011> emitter tip image after weak flashing. a) Tip image. b) Enlarged image in the vicinity of the (010) plane.

The step size shown in Fig. 6 (b) was analyzed as follows. From Fig. 6 (a), the shape of the tip is thought to be like that shown in Fig. 7 (a). As the angle between each crystal plane in the bcc structure are clearly known, the angles between each plane and the primary electron beam in the SEM can be analyzed from the observed image in Fig 6 (a). The result showed that the direction of <011> is tilted about 40° from the beam direction. In addition, the (010) plane is rotated about 15° counter clockwise around <011> as shown in Fig. 7 (b). Then, the chord between (010) and (1̄10) is almost perpendicular to the beam direction. Accordingly, these steps are recognized as double atomic layers (4.5Å) on the (1̄10) plane as shown in Fig. 7 (c), because the step cycle of the (1̄10) plane is about 14Å in width as shown in Fig. 6 (b). It is assumed that these steps become monolayered after complete recrystallization.

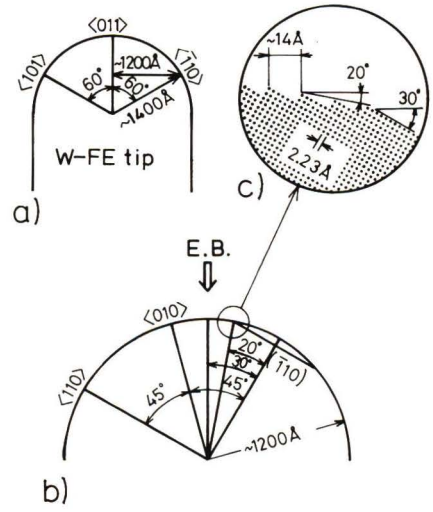

Fig. 7 Schematically analyzed the atomic step in Fig. 6 b). a) External form of the tip as seen in Fig. 6 a). b) Meridian plane containing primary beam. c) Schematic cross-section of atomic structure.

The analysis presented above shows that the SEM has the ability to resolve steps as small as several angstroms, even though the step size is not directly related to the resolution of the SEM.

Ti/W<001> FE Tip

A Ti/W<001> field emitter was developed to confine the electron emission to a relatively small angle. The emitter can be operated at a lower temperature (1500 K) than that (1800 K) of a zirconiated tungsten (Zr/W<001>) field emitter [13]. This emitter also offers the advantages of low beam current drift of 1%/hour and low FE noise.

A single W<001> crystal wire is spot-welded to the apex of a W hair-pin filament wire. Ti wire is then twisted around the filament. The W<001> wire is then electrolytically etched in the same manner as in the conventional FE tip formation process. The Ti wire is melted by direct heating by passing a current through the filament wire in a vacuum chamber. When Ti is diffused by heat treatment in an oxygen atmosphere, an angularly confined FEM pattern is obtained in the thermal field emission (TFE) mode.

The image of the W<001> emitter tip and its FEM pattern are shown in Fig. 8. The crystallographic planes are clearly visible and the FEM pattern corresponding to each plane is clearly defined.

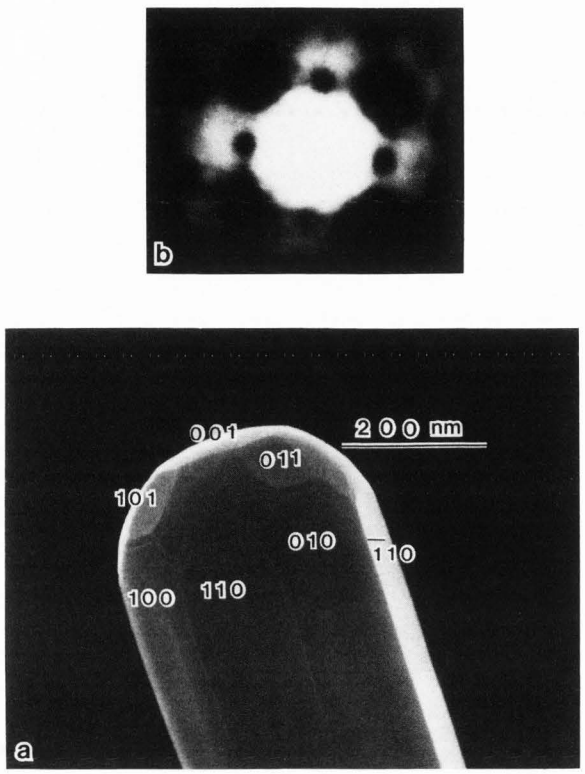

Fig. 8 W<001> FE tip image and its FEM pattern.

The image of the Ti/W emitter tip after thermal diffusion of Ti and its FEM pattern are shown in Fig. 9. The emission is clearly confined in a small area and the shape of the emitter tip is drastically altered. In the Ti/W tip, the shape is hemispherical and the portion corresponding to {100} is circular steps. In addition, the center of the {100} face is seen to be slightly concave. Although it is difficult to determine whether the Ti on the {100} plane is a monolayer or not, it can be assumed that the shape of the tip is due to the fact that Ti is thinly adsorbed on the center of the {100} plane whereas the rest of the emitter is covered with a thick deposit of Ti. As a result, the work function of the {100} plane is lower than that of all other planes. It is therefore thought that this contributes to the angular confinement of the emission current.

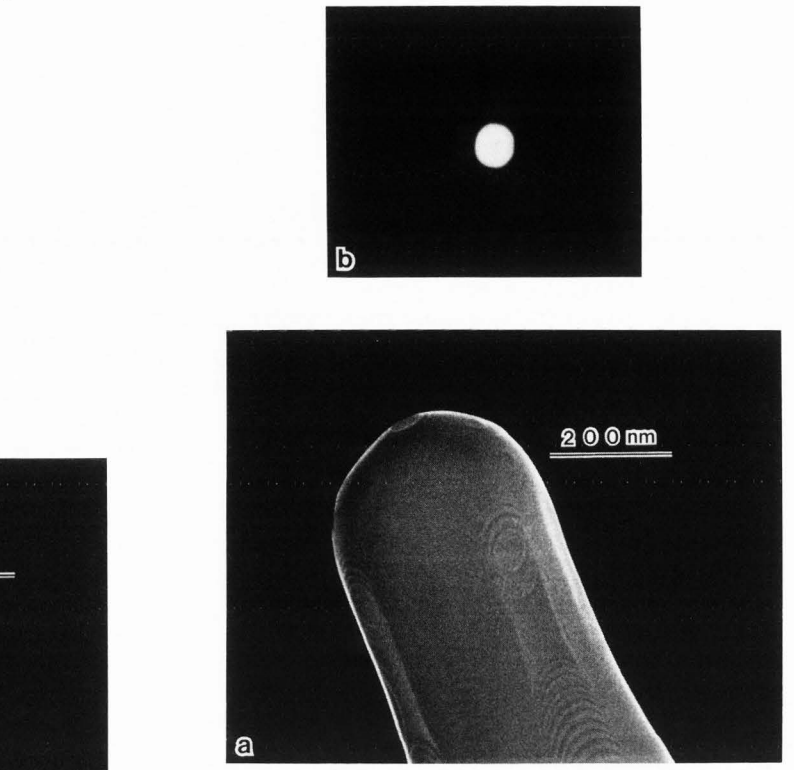

Fig. 9 Ti/W<001> FE tip image and its FEM pattern.

Conclusion

FE tips were observed using a prototype FE-SEM with an in-lens type objective lens. The SEM was shown to be able to resolve atomic layer steps of several angstroms. It was also found that the tip aspect was drastically altered in the Ti/W emitter following thermal diffusion of Ti. Consequently, it was possible to obtain sharp FEM patterns due to confinement of the emission current flowing from the tip.

Acknowlegements

The authors would like to thank Prof. K. Tanaka, Dept. of Anatomy, Tottori Univ., for his fruitful encouragement during the course of the development of the prototype SEM. Thanks are also due to Dr. T. Nagatani, Mr. S. Saitoh, Mr. I. Matsui and their co-workers at Hitachi Ltd's Naka works for their thoughtful discussion on FE-SEM.

References

1) Butler J.W. (1966) Digital Computer Techniques in Electron Microscope , Proc. 6th Int. Cong. Electron Microscopy, I, Kyoto, 191.

2) Crewe A.V., Eggenberger D.N., Wall J. and Welter L.M. (1968) Electron Gun using a Field Emission Source , Rev. Sci. Instrum., 39, 576-583.

3) Hosoki S., Takata K. and Kaga H. (1986) Ti/W(100) Field Emission Source , Proc. XIth Int. Cong. on Elec. Microsc., ICEM, I, Kyoto, (1986) 219-222.

4) Komoda T. Saito S. (1972) Experimental Resolution Limit in The Secondary Electron Mode for A Field Source Scanning Electron Microscope , Scanning Electron Microsc. 1972:129-136.

5) Koshikawa T. and Shimizu R. (1974) A Monte Carlo Calculation of Low-Energy Secondary Electron Emission from Metals , J. Phys.D: Appl. Phys., 7, 1303-1315.

6) Kuroda K. (1974) Analysis and Design of Accelerating Lens System for Field Emission Scanning Electron Microscope , Ph.D. thesis, Osaka Univ. (1974) Dec.

7) Kuroda K. and Hosoki S. (1985) Resolution Limit of Secondary Electron Image , Proc. of the 41th Annual Meeting of Japan Soc. of Elec. Microsc., (1985) 13 (in Japanese).

8) Kuroda K., Hosoki S. and Komoda T. (1985) Observation on Crystal Surface of W<110> Field Emitter Tip by A Scanning Electron Microscope , Jour. Elec. Microsc., 34, 179-182.

9) Nagatani T. and Saito S. (1986) Instrumentation for Ultra-high Resolution Scanning Electron Microscope , Proc. XIth Int. Cong. on Elec. Microsc., ICEM, III, Kyoto, 2101-2104.

10) Nagatani T., Yamada M., Saito S. and Nakaizumi Y. (1983) An Experiment in Ultra-high Resolution SEM , Biomedical SEM, 12, 8-9 (in Japanese).

11) Nagatani T. Okura A. (1977) Enhanced Secondary Electron Detection at Small Working Distance in The Field Emission SEM , Scanning Electron Microsc. 1977;I:695-702.

12) Shimizu R., Kuroda K., Suzuki T., Nakamura S., Suganuma T. and Hashimoto H. (1973) Field Emission Scanning Electron Microscope with Parallel Plate Gun Electrodes , Scanning Electron Microsc. 1973:73-80.

13) Swanson L.W. and Crouser L.C. (1969) Angular Confinement of Field Electron and Ion Emission , J. Appl. Phys., 40, 4741-4749.

14) Tamura H. and Kimura H. (1968) New Method of Detecting Secondary Electrons on Scanning Electron Microscope , Jour. Elec. Microsc., 17, 106-111.

15) Tanaka K., Matsui I., Kuroda K. and Mitsusima A. (1985) A New Ultra-high Resolution Scanning Electron Microscopy (UHS-T1) , Biomedical SEM, 14, 23-25 (in Japanese).

16) Tanaka K. (1981) Demonstration of Intracellular Structures by High Resolution Scanning Electron Microscopy , Scanning Electron Microsc. 1981;I:1-8.

17) Thompson M. (1977) "Discussion with the Reviewers" in: O. C. Wells, Backscattered Electron Image In The Scanning Electron Microscope , Scanning Electron Microsc. 1977;I:747-771.

Discussion with Reviewers

J. Cowley: Can you suggest how the SEM contrast is generated for the small surface steps?
Authors: We aren't sure exactly in detail. We are now attempting to clarify this using a Monte Carlo simulation.

J. Cowley: It has been said that the resolution of a SEM image should be limited not by the probe size but by the delocalization of the inelastic scattering processes giving rise to the secondary electrons. Do you have any evidence for the existence of such a delocalization effect?
Authors: We have no explicit evidence for specimens such as these emitters. In the observation of GaAs superlattice construction, however, we have the impression that the resolution deteriorates, and this deterioration might depend on the delocalization effect.

M. Gesley: Why can the Ti/W emitter be operated at a lower temperature than the Zr/W cathode?
Authors: The melting point of Ti is lower and it is easier to diffuse than Zr. As a result, the Ti/W emitter can be operated at a lower temperature.

M. Gesley: Under what oxygen partial pressure and for what time duration is the emitter heated to obtain angular confinement of the emission current?
Authors: When making a tip, the partial pressure needed during heat treatment is 1.3×10^{-5} Pa and the thermal diffusion time

is about 30min at about 1800K. In the emission mode an oxygen ambient is not needed.

M. Gesley: Re summary paragraph, the last paragraph in section "Observation for Tungsten FE-Tips" and comments in abstract: It may be worthwhile to more clearly distinguish between lateral and step size resolution, e.g. scanning confocal optical microscopy can also resolve angstrom-scale step resolution without approaching the lateral resolution of the SEM. This paper has not directly demonstrated 5Å lateral resolution, which is predicted, but only 14Å.
Authors: You are right. This is not described anywhere in this paper. In Ref. 7, however, we demonstrated approximately 5Å lateral resolution from the minimum separate distance of platinum particles coated on a biological specimen.

J. Orloff: It would be of interest to know what the scan time is for your high resolution micrographs, and what the current and noise figures are for the focused beam. Also, it appears that the final beam aperture in the objective lens is actually the image of the aperture which is located near the anode. If this is so, how good a job does it do in preventing stray electrons from reaching the target, or are other apertures used as well? Finally, how much contribution to the final beam size is there from the Butler lens, the aberrations of which will become appreciable as $V_{beam} \rightarrow V_{extraction}$?
Authors: The scan time is 100sec. and the beam current is on the order of 10^{-11}A. There is another aperture, which is located at the center of the condenser lens, to prevent the electrons from being scattered by the edge of the limiting aperture. The aberration of the Butler lens is reduced by the demagnification of the condenser and objective lenses, and is estimated to be less than 1Å.

M.G.R. Thomson: Does the detector respond to high energy backscattered electrons in addition to secondary electrons? Is there any difference in the observed resolution in these cases?
Authors: As the backscattered electrons (B.E.) have a high energy, they are not deflected to the detector by the electric field of the detector. Therefore, they are not detected. If B.E.'s are detected in addition to S.E.'s, the resolution would be slightly deteriorated, because B.E.'s are emitted from deeper and wider portions of the specimen than S.E.'s. Nagatani and his co-workers in Hitachi's Naka works observed the B.E. and S.E. images of lead-evaporated particles using a Hitachi S-900 SEM and showed that the difference in resolution was not significant.

M.G.R. Thomson: Is there any other evidence that the surface of the Ti/W emitter tip contains adsorbed titanium? Is there any evidence that this layer varies in thickness in different areas? Is oxygen also present?
Authors: This was confirmed by analyzing atoms on an emitter surface using an atom probe FIM. The mass analysis revealed, in order, the presence of Ti, TiO+WO and W. Accordingly, Ti and oxygen are present without fail. The measured amount of Ti corresponds to about one monolayer in a detailed analysis.